

## A Size-controlled Synthesis of Hollow Apatite Nanospheres at Water–Oil Interfaces

Wenhui He, Jinhui Tao, Haihua Pan, Xurong Xu, and Ruikang Tang\*

Department of Chemistry and Center for Biomaterials and Biopathways, Zhejiang University, Hangzhou 310027, P. R. China

(Received March 23, 2010; CL-100281; E-mail: rtang@zju.edu.cn)

A size-controllable synthesis of hollow structures of apatite in the hexane–water–bis(2-ethylhexyl) sulfosuccinate is presented, and the hollow sphere sizes can be easily regulated within a range of 50–1000 nm. The isotherm curves of the size controls and the roles of different experimental parameters are discussed. This feasible pathway may offer an ideal strategy of the size-controlled synthesis of hollow nanomaterials.

There is intense interest in a simple and general strategy to synthesize hollow-structured nanospheres due to their unique structures and properties. Various approaches have been studied by using different methods such as colloidal/microemulsion templates, sonochemistry, and hydrothermal synthesis,<sup>1</sup> among them liquid–liquid interfaces in microemulsion offer suitable scaffolds for in situ synthesis of nanosized materials. Because of the simplicity and the dynamic properties, this liquid–liquid method always results in the formation of superstructure with fewer defects.<sup>2</sup> As an important biomineral, apatite has attracted a great deal of attention since it is a main component of hard tissues of vertebrates. Apatite has many applications such as in biological implants,<sup>3</sup> separation of proteins and nucleic acids, removal of heavy-metal ions, and as carrier for catalysts.<sup>4</sup>

Hollow-structured nanospheres of apatite may serve important functions as drug carriers and diagnostic markers.<sup>5</sup> There are several strategies for the preparation of calcium phosphate nanospheres such as plasma spray,<sup>6</sup> liposome-directed mineralization,<sup>5</sup> polymer micelle/nanocage-templated precipitation,<sup>7</sup> and microemulsion.<sup>8</sup> However, these methods have poor control of particle size. For example, liposomes are an effective template for nanoshells, and calcium phosphate can precipitate on the exterior walls, but the sizes of obtained nanospheres are limited to within tens of nanometers. By using polymer micelles of polyacrylic acid, the typical sizes of obtained calcium phosphate range from 50 to 80 nm. Although hollow apatite spheres can be prepared by plasma spray, the sizes are as large as several micrometers. Actually, the size control of nanospheres is a great challenge in current nanomaterial research. It is emphasized that an approach to a size-controlled synthesis of hollow-structured apatite has not been reported. In the present work the oil-in-water microemulsion in the hexane–water–bis(2-ethylhexyl) sulfosuccinate (AOT) system is applied to the synthesis of hollow apatite spheres. The sizes of the obtained materials can be easily regulated within a range of 50–1000 nm. In the experiments, an aqueous disodium hydrogen phosphate solution and hexane were used as the continuous and dispersed phase in the oil-in-water system, respectively. Other compounds, Ca(AOT)<sub>2</sub> (Figure S1) and NaAOT (molar ratio of Ca:Na was 1:5), were used as the surfactant to stabilize the oil phase, in which Ca(AOT)<sub>2</sub> also provided the calcium ions for the apatite formation.

The controllable synthesis was performed in the L1 zone in the phase diagram of water–hexane–AOT. L1 zone indicated that

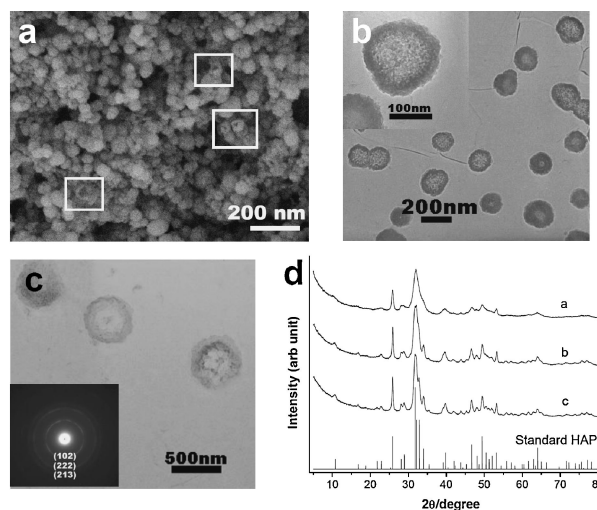


**Figure 1.** (a) SEM of  $60 \pm 10$  nm apatite spheres; the hollow structures could be observed by some broken spheres (rectangles). TEM of different hollow spheres of apatite, (b)  $180 \pm 20$  and (c)  $500 \pm 20$  nm; the inserts are enlarged images or SEAD pattern. (d) Corresponding XRD patterns of the as-prepared samples in (a), (b), and (c).

the relatively stable oil-in-water microemulsion was present<sup>9</sup> so that the apatite precipitation could occur at the oil–water interface. Interestingly, the sizes of the achieved hollow apatite spheres were dependent upon the experimental parameters. Scanning electron microscopy (SEM) and transmission electron microscopy (TEM) images (Figure 1) showed that the sizes monotonically increased from tens of nanometers up to one micrometer.  $60 \pm 10$  nm nanospheres were obtained under oil/water and oil/AOT ratios of  $6.84 \times 10^{-4}$  and 0.0932, respectively. Different experimental conditions and results are summarized in Table S1.<sup>11</sup> It was found that the influence of AOT content on the size regulation was not so significant within the L1 zone. However, with the increase of oil ratio in the water–hexane–AOT system, the sizes of nanospheres increased accordingly.  $180 \pm 20$ ,  $500 \pm 20$ , and  $900 \pm 100$  nm nanospheres were obtained at the oil/water ratios of 0.0018, 0.0042, and 0.0054, respectively. The selected area electron diffractions (SAED) corresponded to typical apatite lattice structures, which were different from the amorphous structures reported in the previous literature.<sup>5,7,8</sup> The apatite formations were also confirmed by the X-ray diffraction (XRD) studies. The patterns matched the standard one (JCPDS 09-0432) well. The thickness of the shells was relatively uniform despite the different sphere structures, which was about 15 nm. The isotherm curves of the size controls are shown in the phase diagram of water–hexane–AOT (Figure 2a). The curves were

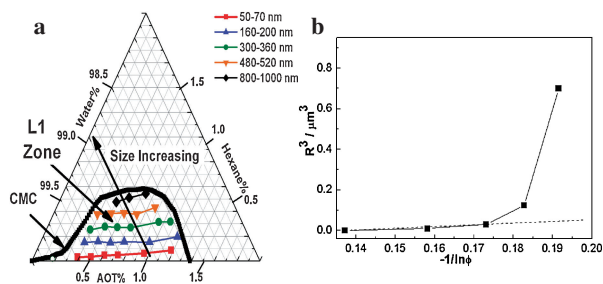


**Figure 2.** (a) Phase diagram of hexane–water–AOT. The sizes of the hollow apatite spheres were marked with the experimental parameters in the L1 zone and the isotherm curves of the size controls were achieved. (b) Curve of  $R^3$  vs.  $-1/\ln\phi$ . When the term of  $-1/\ln\phi$  was less than 0.18, the experimental dots are almost in a straight line as shown in eq 1.

almost parallel to the baseline of the phase diagram, which clearly indicated the important role of oil/water ratio in the size regulation. These curves could provide guidance for the controllable synthesis of hollow apatite spheres.

In the L1 zone, the hexane phase was dispersed in water, and the surfactant, AOT, acted as stabilizer for the oil-in-water microemulsions. AOT had a hydrophilic group,  $-\text{SO}_3^-$  and two alkyl hydrophobic chains. In the stable configuration of the AOT in the L1 zone, its hydrophilic group pointed to the water phase and the hydrophobic group immersed in hexane phase. Calcium ions were electrically attracted by the  $-\text{SO}_3^-$  functional group, resulting in a Stern layer on the oil–water interface. While the diffuse layer mainly consisted of the added phosphate ions, the local supersaturation of calcium phosphate at the oil–water interfaces was great, which led to in situ crystallization of apatite.<sup>5,7</sup> This reaction finally resulted in the formation of apatite shells with oil cores. In the preparation, the oil-in-water structure in L1 zone was an important template in the formation of hollow apatite spheres. If the synthesis was performed at any point out of this zone, the obtained solids were needle-like nanopatite crystallites, which were similar to the conventional formations without the template effects (Figure S2).<sup>11</sup>

The hollow structures of apatite were dependent upon the oil droplets, and their sizes could be modulated by the ratio of oil phase to aqueous solution. As the Ostwald theory depicted by Yao et al.,<sup>10</sup> the average droplet radius  $R$  could be described as a function of the volume fraction of droplet phase in the continuous phase,  $\phi$ . In the limit condition of  $\phi \rightarrow 0$ , the relationship between  $R$  and  $\phi$  could be simplified as eq 1,

$$R^3 = A - B/\ln\phi \quad (1)$$

where  $A$  and  $B$  were the constants, determined by nature of the phase materials. The equation indicated that an increasing oil/water ratio would result in larger hollow structures. Although eq 1 fitted the experimental results when  $\phi < 0.003$  due to the limit condition of  $\phi \rightarrow 0$  (Figure 2b), the curves could be still useful in the design of synthesis conditions for hollow apatite nanospheres with any required sizes.

A peanut-like structure was also detected (Figure 1b) in the synthesis. This appearance could be understood by the collision of oil droplets (Figures 3a and 3b). Actually, the peanut-like structure could be used to monitor the growth and coagulation of the separated oil droplets, and it is also an indication of the

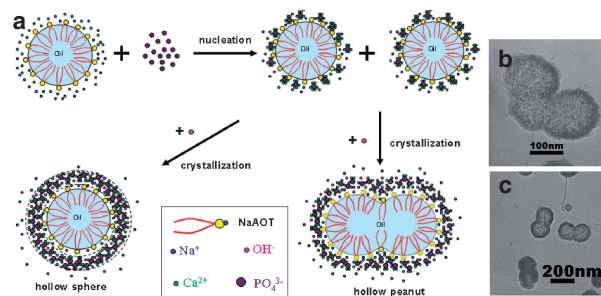


**Figure 3.** Schematic illustration of in situ mineralization of apatite at the oil–water interface. The synthesis of hollow spheres was templated by a single oil droplet in the L1 zone. The collision and partly coagulation of the droplets resulted in the peanut-like structures.

flexible interface between oil and water. We found that the content of AOT actually could influence the morphology of the samples. When the size of spheres increased with an increase of hexane content, the average value of hexane/AOT weight ratio raised accordingly. Without further addition of AOT, the stabilizer, the stability of oil droplets in aqueous phase was decreased and the collision was promoted. As a result, when the experimental conditions were similar, more peanut-like structures were induced at the lower AOT content (Figure 3c).

In summary, we proposed a convenient strategy of size-controlled synthesis of hollow apatite spheres in this study. By using our method, the control of nanoparticle sizes within a range of 50–1000 nm could be easily achieved.

#### References and Notes

- a) B. L. Cushing, V. L. Kolesnichenko, C. J. O'Connor, *Chem. Rev.* **2004**, *104*, 3893. b) U. Jeong, Y. Wang, M. Ibisate, Y. Xia, *Adv. Funct. Mater.* **2005**, *15*, 1907. c) M. J. MacLachlan, I. Manners, G. A. Ozin, *Adv. Mater.* **2000**, *12*, 675. d) S. A. Johnson, P. J. Ollivier, T. E. Mallouk, *Science* **1999**, *283*, 963. e) K. P. Velikov, A. van Blaaderen, *Langmuir* **2001**, *17*, 4779. f) N. A. Dhas, K. S. Suslick, *J. Am. Chem. Soc.* **2005**, *127*, 2368. g) F. Caruso, *Chem.—Eur. J.* **2000**, *6*, 413.
- a) Y. Lin, H. Skaff, T. Emrick, A. D. Dinsmore, T. P. Russell, *Science* **2003**, *299*, 226. b) A. D. Dinsmore, M. F. Hsu, M. G. Nikolaidis, M. Marquez, A. R. Bausch, D. A. Weitz, *Science* **2002**, *298*, 1006. c) W. H. Binder, *Angew. Chem., Int. Ed.* **2005**, *44*, 5172. d) H. W. Duan, D. Y. Wang, D. G. Kurth, H. Möhwald, *Angew. Chem., Int. Ed.* **2004**, *43*, 5639.
- Y. J. Wu, S. Bose, *Langmuir* **2005**, *21*, 3232.
- a) T.-G. Kim, B. Park, *Inorg. Chem.* **2005**, *44*, 9895. b) Y. Matsumura, S. Sugiyama, H. Hayashi, N. Shigemoto, K. Saitoh, J. B. Moffat, *J. Mol. Catal.* **1994**, *92*, 81. c) R. Ramesh, R. Jagannathan, *J. Phys. Chem. B* **2000**, *104*, 8351. d) H. Takeda, Y. Seki, S. Nakamura, K. Yamashita, *J. Mater. Chem.* **2002**, *12*, 2490. e) G. Adachi, N. Imanaka, S. Tamura, *Chem. Rev.* **2002**, *102*, 2405.
- a) H. T. Schmidt, B. L. Gray, P. A. Wingert, A. E. Ostafin, *Chem. Mater.* **2004**, *16*, 4942. b) H. T. Schmidt, A. E. Ostafin, *Adv. Mater.* **2002**, *14*, 532.
- a) R. X. Sun, M. S. Li, Y. P. Lu, S. T. Li, *Mater. Res. Bull.* **2006**, *41*, 1138. b) R. X. Sun, Y. P. Lu, M. S. Li, *Surf. Eng.* **2003**, *19*, 392.
- K. K. Perkin, J. L. Turner, K. L. Wooley, S. Mann, *Nano Lett.* **2005**, *5*, 1457.
- C. E. Fowler, M. Li, S. Mann, H. C. Margolis, *J. Mater. Chem.* **2005**, *15*, 3317.
- C. L. Mesa, L. Coppola, G. A. Ranieri, M. Terenzi, G. Chidichimo, *Langmuir* **1992**, *8*, 2616.
- a) J. H. Yao, K. R. Elder, H. Guo, M. Grant, *Phys. Rev. B* **1993**, *47*, 14110. b) N. D. Alikakos, G. Fusco, *J. Stat. Phys.* **1999**, *95*, 851.
- Supporting Information is available electronically on the CSJ-Journal Web site, <http://www.csj.jp/journals/chem-lett/index.html>.